

PAPER • OPEN ACCESS

Microstructure evolution and residual stress changes of the GH4169 alloy by wet shot peening

To cite this article: P F Zhou *et al* 2019 *IOP Conf. Ser.: Mater. Sci. Eng.* **563** 022040

View the [article online](#) for updates and enhancements.

Microstructure evolution and residual stress changes of the GH4169 alloy by wet shot peening

P F Zhou, H Z Zheng*, S H Guo, S P Cheng, G F Li

National Defense Key Disciplines Laboratory of Light Alloy Processing Science and Technology, Nanchang Hangkong University, Nanchang 330063, P.R. China.

*Corresponding author Tel: +86 791 86453207; E-mail address: zhznchu@126.com

Abstract. GH4169 alloy was shot-peened with processing durations of 3 min and 10 min. The effects of dry and wet shot peening on the microstructure and residual stress were investigated. The results demonstrated that a severely deformed layer manifests on the surface of the shot-peened GH4169 alloy samples. Compared with the dry-peening samples, the surface defects of wet-peening samples obviously decrease. With the shot peening treated for 10 min, the surface microhardness of the dry peening and the wet shot peening increased by 20% and 17% respectively compared with the original surface hardness. The deformation mechanisms of the GH4169 alloy could be attributed to dislocation and deformation twinning, as detected by TEM observations. Compressive residual stress was introduced into the surface layer of the shot-peened GH4169 alloy. The maximum surface residual compressive stress (SRS) and maximum residual compressive stress (MRS) were -586 MPa and -795 MPa, respectively. The MRS and SRS were improved with increasing processing duration. The SRS of the wet-treated specimens was slightly higher than that of the dry-treated samples under the same processing parameters. However, the MRS of dry-treated samples was much larger than that of the wet-treated samples due to the higher shot intensity.

1. Introduction

Ni-based superalloys, such as the GH4169 alloy, are widely used in high-temperature fields, especially space navigation, due to their excellent radiation resistance, corrosion resistance, good machinability, and welding performance.^[1-3] However, the GH4169 alloy can no longer meet the demands of rapidly developing aviation industry as the fatigue strength and fretting fatigue resistance of nickel-based alloys are insufficient. Therefore, further improvements to the properties of GH4169 alloy are needed in order to ensure it maintains its widespread application.

Dry shot peening, as a conventional strengthening process, is widely used for modifying the microstructure and improving the mechanical properties of metals and alloys. Gao et al.^[4] studied the fatigue life of 7475-T7351 aluminum alloy subjected to shot peening. The results demonstrated that the fatigue life of a treated aluminum alloy is greatly extended because of the beneficial compressive residual stresses induced in the surface layer. Fridrici et al.^[5] reported that shot peening has a beneficial effect on the fretting fatigue resistance of treated Ti-6Al-4V alloy by inhibiting crack initiation and propagation under fretting wear loading. However, dry shot peening often results in high surface roughness on the treated surface, which is unfavorable for the functionality of the treated components. High surface roughness has been shown to reduce fatigue strength, facilitate crack initiation under fatigue loading, and increase the natural scatter of the field strength of the materials.^[6-9] Therefore, high surface roughness needs to be minimized when considering the improvement of



fatigue strength during shot peening.

As the surface-strengthening technology rapidly develops, wet shot peening ensures the use of shots placed in liquids (water or oil) containing a certain amount of corrosion inhibitors. As opposed to dry shot peening, wet peening is conducive to obtaining a lower surface roughness and yields better surface quality due to the formation of a liquid film on the component surface, which effectively reduces friction and cools the surface. At the same time, the service life of nozzles and projectiles are improved due to the lubrication and cooling of the liquid medium. In addition, wet shot peening can reduce the noise and dust pollution in the working environment and provide a good working environment. Chen et al.[10] studied the effects of wet shot peening on Ti-6Al-4V alloy and showed that samples treated with wet shot peening have surface roughness of an order of magnitude lower than that of dry shot-peened samples. Takemoto[11] studied the effects of wet shot peening on the residual stress improvement of welded pipes. His results illustrated that the compressive stress induced by wet shot peening is larger than that induced by dry shot peening due to the conjoint effects of thermal stress caused by water cooling and shot peening. Sekoda and Tosha[12] reported that the fatigue strength of the medium carbon steel was improved by 20% after wet peening. To date, the wet shot peening of the GH4169 alloy has not been reported. In this paper, emphasis is given to the effects of wet shot peening on the microstructure evolution and residual stress changes of the GH4169 alloy. The results are compared with those obtained by dry shot peening.

2. Experimental procedures

The material used is GH4169 alloy with chemical composition (in wt.%) of 0.039% C, 0.001% S, 0.11% Si, 52.38% Ni, 18.61% Cr, 2.98% Mo, 0.96% Ti, 4.94% Nb, 0.0079% Mn, 0.005% P, 0.56% Al and balance Fe. The as-received alloy was annealed at 960 °C for one hour and then cooled to 30°C in air. As shown in **Figure 1**, the microstructure of the GH4169 alloy is uniform, and the average grain size is about 100 μm , with a few annealing twins inside the grains (indicated by arrows).

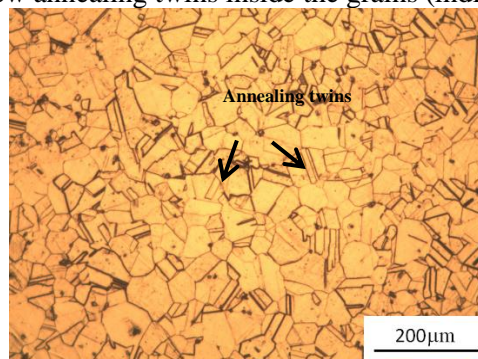


Figure 1. The microstructure of as-annealed GH4169 alloy.

Shot peening samples with dimensions 8 mm \times 8 mm \times 5 mm were manufactured from the as-annealed GH4169 alloy. The sample surfaces were ground using 600 to 2000 grade waterproof sandpaper and then mechanically polished with 1, 3 and 5 grade diamond paper before shot peening. Two types of shot peening were employed, namely, dry shot peening and wet shot peening. Wet shot peening was performed on an air-blasting machine using a compound of shots and water with a volume ratio of 1:3. The GH4169 alloy samples were treated using cast steel shots with a diameter of 1.0 mm at a pressure of 0.7 MPa and processing durations of 3 min and 10 min. The angle and the distance between the shot nozzle and the specimens were approximately 90° and 550 mm, respectively.

To investigate the microstructure evolution after the shot peening treatment, cross sections of the specimens were prepared for metallographic examination by mechanical polishing, followed by chemical etching with 10 g CuSO_4 + 50 mL HCl + 10 mL HF + 30 mL HNO_3 . The cross-sectional microstructure analysis was performed with optical microscopy (OM) and QUANTA 200 scanning electron microscopy (SEM) at a voltage of 20 kV. The microhardness was measured using a HVS-1000 digital microhardness tester with an accuracy of 1 Vickers (the force of 200 g to the

specimen for 20 s). The microstructure of the treated surface layer was characterized by JEOL JEM-2100 transmission electron microscopy (TEM) at an operating voltage of 200 kV. The phase composition of the GH4169 alloy samples was determined by X-ray diffraction (XRD, D8 ADVANCE) with Cu K α radiation ($\lambda = 1.54183 \text{ \AA}$), operating at 40 kV and 20 mA. The scanning speed was $0.02^\circ/\text{s}$. The surface roughness (R_a) was measured at three different locations to obtain the average roughness by using a JB-6CA surface profiler. A three-dimensional non-contact optical profilometer (ZYGO NewView 5022) was used to observe the 3D contour profiles of shot-peened specimens. The residual stresses of the treated samples were investigated by an X-ray $\sin 2\psi$ stress analyzer (LXRD, Proto, Canada, X-ray tube type: Mn-K α (V-filter) a diffraction plane: (311), a tube voltage of 30 kV, a tube current of 25 mA, an incident slit with $\Phi = 2 \text{ mm}$, and 2 Theta degree of 20°). In addition, subsurface stress measurements were conducted after successive layers were removed by electrolytic polishing.

3. Results

3.1 Cross-sectional microstructure observation

The cross-sectional optical micrographs of the shot-peened GH4169 alloy are shown in **Figure 2**. Unlike the matrix microstructure, the surface layer microstructure changes gradually from severely deformed grains to un-deformed grains in the matrix, and the grain boundaries in the severe plastic deformation layer cannot be identified by OM observation. Compared with the cross-sectional microstructures of the GH4169 alloy treated for 3 and 10 min, the experiments revealed that the thickness of the deformed layer increases with increasing the processing time. The deformed layer thicknesses of the dry shot-peened specimens were $85 \text{ }\mu\text{m}$ (3 min) and $200 \text{ }\mu\text{m}$ (10 min), which were slightly higher than those of the wet shot-peened samples ($80 \text{ }\mu\text{m}$ (3 min) and $185 \text{ }\mu\text{m}$ (10 min)). Furthermore, the surface flatness of the dry shot-peened samples with 10 min processing duration (**Figure 2(c)**) was much lower than that of the wet shot-peened samples (**Figure 2(d)**). This may be attributed to the numerous craters created on the surface layer, as the high-speed impact of shots was against the sample surface.

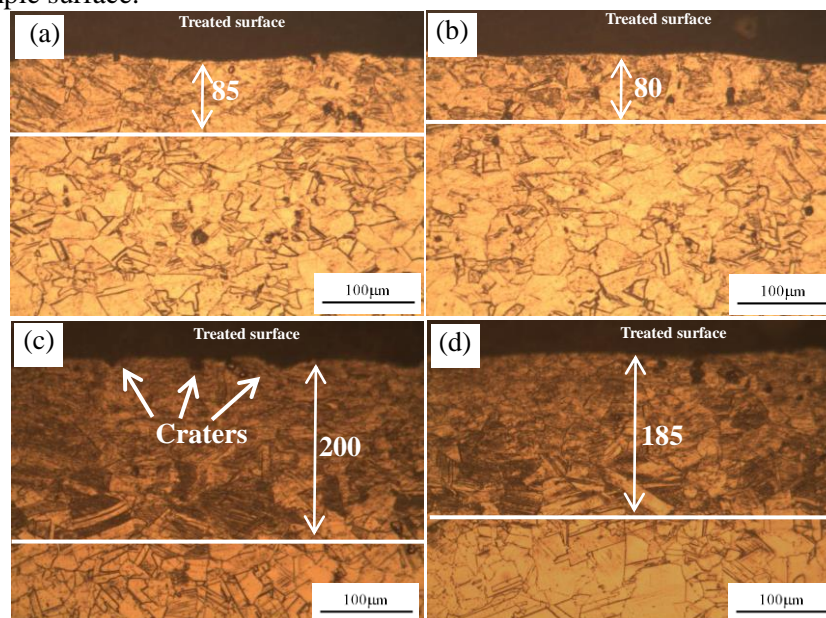


Figure 2. Cross-sectional metallurgical micrographs of shot-peened GH4169 alloy (a) dry shot-peened for 3 min, (b) wet shot-peened for 3 min, (c) dry shot-peened for 10 min, (d) wet shot-peened for 10 min.

As per the literature,[13-14] phase transitions occasionally occur with severe plastic deformation. The primary phases identified by XRD on the surface of as-annealed and shot-peened GH4169 alloy are plotted in Figure 3. The Bragg diffraction peaks of the as-annealed samples correspond to austenite

γ (111), γ (200), and γ (220). The observed diffractograms from both dry and wet shot-peened specimens fit well with the spectrum of the as-annealed sample (containing the austenite γ phase), indicating that no new phases are formed during severe plastic deformation.

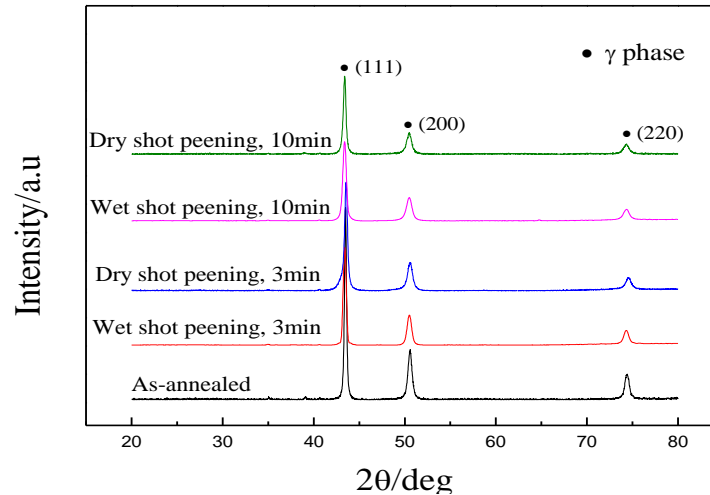


Figure 3. XRD patterns of the untreated and shot-peened GH4169 alloy specimens.

Many recent investigations have used XRD in order to characterize microstructures and strain changes in metals and alloys. Unal et al.[15] have utilized XRD and FWHM (full width at half-maximum) analysis to study the microstructure transformation of AISI304 austenitic steel when it is subjected to shot peening. As illustrated in Figure 3, the peak FWHM of the shot-peened samples are broader and larger compared with the case of the untreated samples due to the crystallite size refinement. The results of XRD analysis strongly confirm those derived from the microscopic analysis (Figure 2). Generally speaking, the broadening of XRD diffraction peaks, the decrease in peak intensity, and the increase in FWHM can qualitatively represent grain refinement: the higher the FWHM, the better the refined microstructure.

As shown in Figure 3 the peaks of the shot-peened GH4169 alloy are slightly broader than that of the as-annealed samples, while the peak intensities are much lower. The γ (111) and γ (200) peak are selected for the analysis of FWHM variations during shot peening, and the results are listed in Table 1. The table shows that the FWHM values of the shot-peened samples are improved. Additionally, the FWHM increases with an increment in the processing time, implying that the degree of microstructure refinement is improved. This corresponds well with the results of microstructure observations. Furthermore, the FWHM of the wet-peened samples is slightly smaller than that of the dry-peened samples, demonstrating that surface plastic deformation of the dry-peened samples might be severer than that of the wet-peened samples.

Table 1. FWHM and 2θ values of shot-peened GH4169 alloy.

GH4169 alloy	Peak	2-the(°)	FWHM	Peak	2-the(°)	FWHM
As-annealed	γ (111)	43.491	0.277	γ (200)	50.604	0.486
Wet shot-peened for 3 min	γ (111)	43.409	0.309	γ (200)	50.501	0.512
Dry shot-peened for 3 min	γ (111)	43.409	0.362	γ (200)	50.563	0.556
Wet shot-peened for 10 min	γ (111)	43.409	0.401	γ (200)	50.481	0.618
Dry shot-peened for 10 min	γ (111)	43.553	0.414	γ (200)	50.481	0.675

3.2 Surface morphology and roughness

The surface morphology and 3D contour plots of surface roughness of as-annealed GH4169 alloy are presented in Figure 4. The surface of the GH4169 alloy before shot peening is quite smooth and the surface roughness is very small. R_a is measured as 0.247 μm .

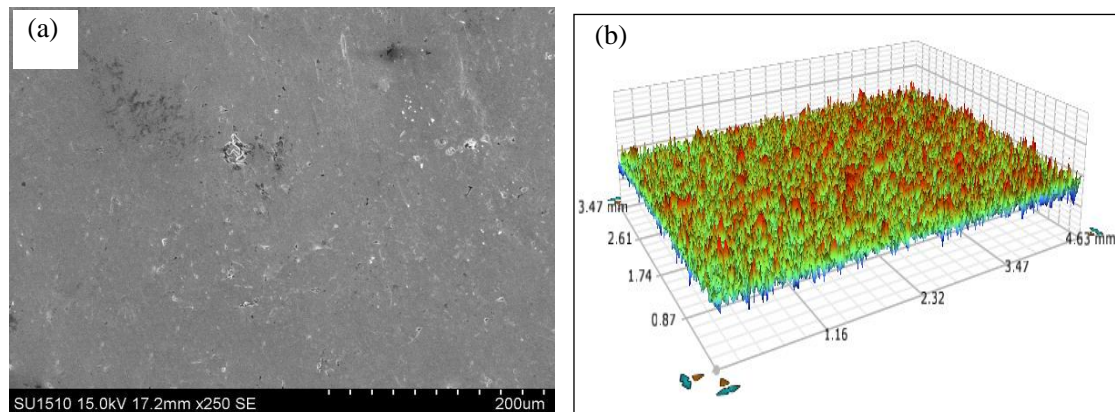


Figure 4. Surface morphology and 3D contour of surface roughness of untreated GH4169 alloy.

Figure 5 and 6 present the surface morphology and 3D contour plots of surface roughness of the shot-peened GH4169 alloy, respectively. As seen from Figure 5(a), the surface of the sample subjected to dry shot peening for 3 min becomes uneven. Pile-ups and flake bulging are generated on the surface due to the high-speed impact of multiple shots. The craters on the sample surface in Figure 6(a) demonstrate that full surface coverage is reached in 3 min. The surface morphology of the dry-peened samples for 10 min is shown in Figure 5(b). A longer processing duration results in the occurrence of a subsidence zone on the surface layer, which may be caused by the peeling off of the flake bulging. As shown in Figure 6(b), the surface is marginally more uneven compared with that of the sample dry treated for 3 min and the R_a value increases to $2.115\text{ }\mu\text{m}$. In contrast with dry shot peening, wet shot peening is conducive to obtaining better surface quality. As shown in Figure 5(c), no obvious pile-ups and flake bulging are observed on the surface of the samples wet treated for 3 min, and the surface flatness (Figure 6(c)) is much higher than that of the dry treated samples. Increasing the treatment duration to 10 min (Figure 5(d)), leads to the surface becoming more uneven and the occurrence of flake bulging. However, there is no subsidence zone on the treated surface, which means that the surface is well protected from the projectile bombardments arising from the lubrication and buffering effects of water during wet shot peening. This results in an obvious decrease in surface roughness ($1.167\text{ }\mu\text{m}$), as shown in Figure 7.

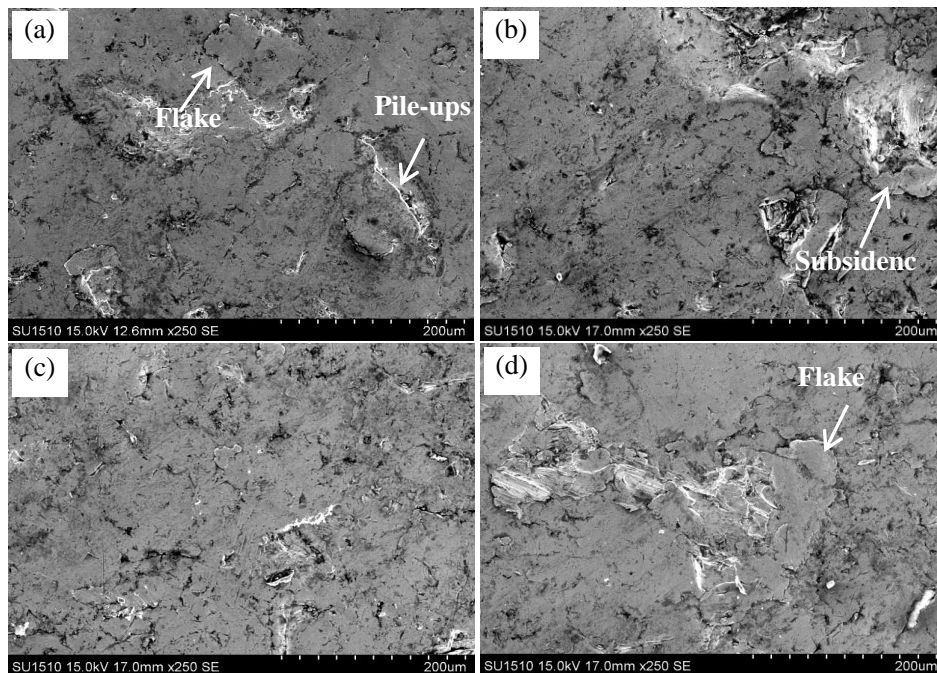


Figure 5. Surface morphology of shot-peened GH4169 alloy (a) dry shot-peened for 3 min, (b) dry shot-peened for 10 min, (c) wet shot-peened for 3 min, (d) dry shot-peened for 10 min.

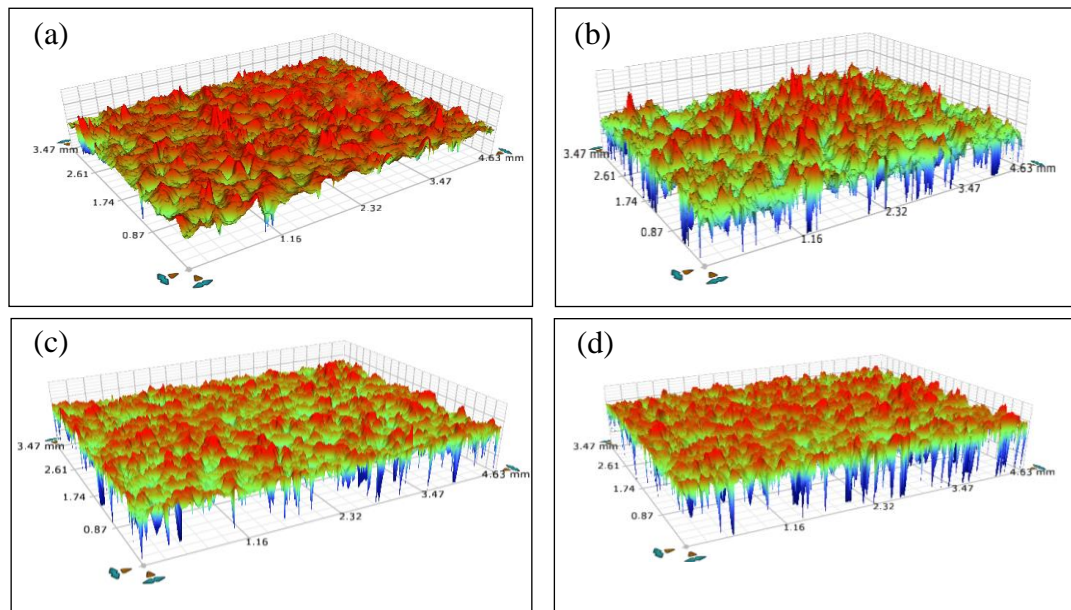


Figure 6. 3D contour of surface roughness of shot-peened GH4169 alloy (a) dry shot-peened for 3 min, (b) dry shot-peened for 10 min, (c) wet shot-peened for 3 min, (d) wet shot-peened for 10 min.

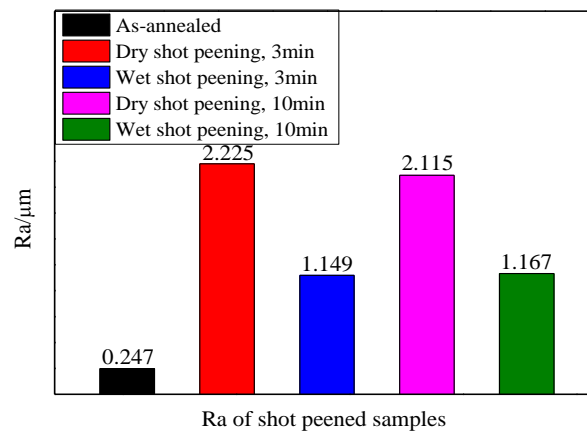


Figure 7. The surface roughness values R_a (μm) of GH4169 alloy specimens after shot peening.

3.3 Microhardness

Figure 8 shows a hardness profile plot for each shot-peening intensity that began close to the shot-peened edge and ended between 450 and 500 μm away from the edge. Compared with the original sample hardness (289 HV), the microhardness is obviously increased. With the shot peening time prolonged, the microhardness of the surface layer is increasing. The surface microhardness of the sample treated with wet shot peening is significantly lower than that of dry shot peening in **Figure 8**. When shot peening was processed for 10 min, the surface cumulative strain energy increased, the surface microhardness increased to 345 HV (dry shot peening) and 338 HV (wet shot peening), and the lifting range reached 20% and 17% respectively.

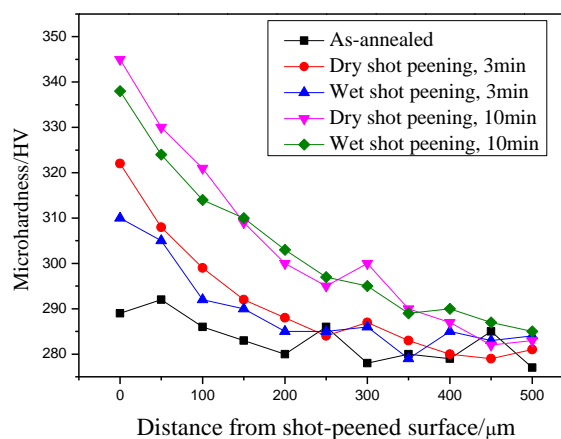


Figure 8. Variation of microhardness with depth of GH4169 alloy samples.

3.4 Residual stress

The residual compressive stress field characteristics introduced by shot peening treatment are summarized by four characteristic parameters: surface residual compressive stress (SRS), maximum residual compressive stress (MRS), depth of the residual compressive stress field (Z_0), and the distance of the location of the maximum residual stress from the surface (Z_m). Figure 9 illustrates the distribution of the residual stresses beneath the surface under different conditions. A residual compressive stress field exists on the surface of all the shot-peened specimens; the residual compressive stresses increase to the peak value and then decrease. As shown in Figure 9, the SRS and

MRS correlate positively with the processing time. The maximum SRS and MRS are -586 MPa and -795 MPa, respectively. In addition, the SRS of the wet-treated specimens is slightly higher than that of the dry-treated samples for the same processing parameters. This may be attributed to the higher roughness of the surface layer of the dry-treated samples, which results in the relaxation of residual compressive stress. Z0 is approximately 300 μm and Zm appears in the subsurface for the shot peened specimens (50~100 μm).

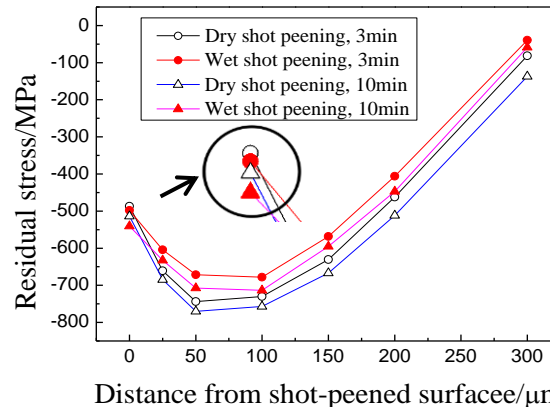


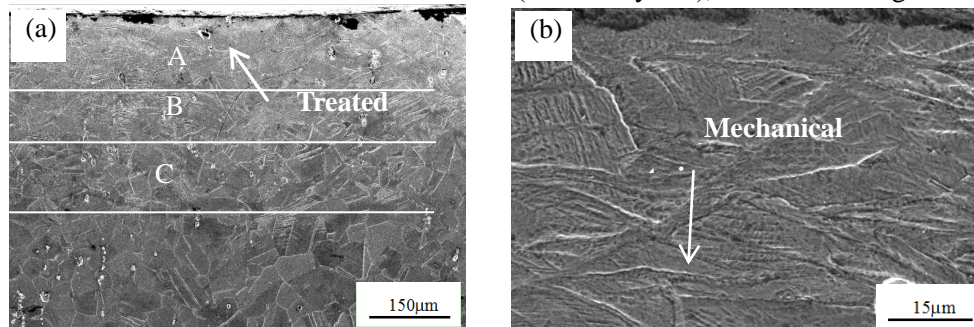
Figure 9. Curves of residual stress distribution of GH4169 alloy after shot peening treatment.

4. Discussion

4.1 Microstructure evolution

According to OM observation (Figure 2), the grain boundaries become ambiguous after shot peening, and the deformed layer thickness increases with increasing processing time. As reported in the literature,^[16] a surface layer with indistinguishable boundaries is considered to be an ultrafine grain layer. During the randomly directed collisions of the cast steel balls with the alloy surface, the kinetic energy of the shot is transformed into strain energy, which then accumulates in the surface layer of the treated samples. The strain energy correlates directly with the processing duration. As the processing time increases, the strain energy increases, resulting in a higher level of deformation and a thicker plastic deformation layer on the surface.

Figure 10 shows the cross-sectional SEM observation of a wet-treated sample with a processing duration of 10 min. A severely deformed layer is formed on the treated GH4169 alloy surface and a mass of mechanical twins and twin intersections can be observed. Prismatic blocks and blocks of other shapes (marked by 'A') are formed in the upper surface layer, which, of course, resulted from the intersections of the mechanical twins in multiple directions (Figure 10(b)). In the deeper layers, rhombic blocks (marked by 'B') are developed by the intersections of two-directional mechanical twins (Figure 10(c)). One-directional parallel mechanical twins are formed in the deeper layers, leading to twin-matrix alternative lamellar structures (marked by 'C'), as shown in Figure 10(d).



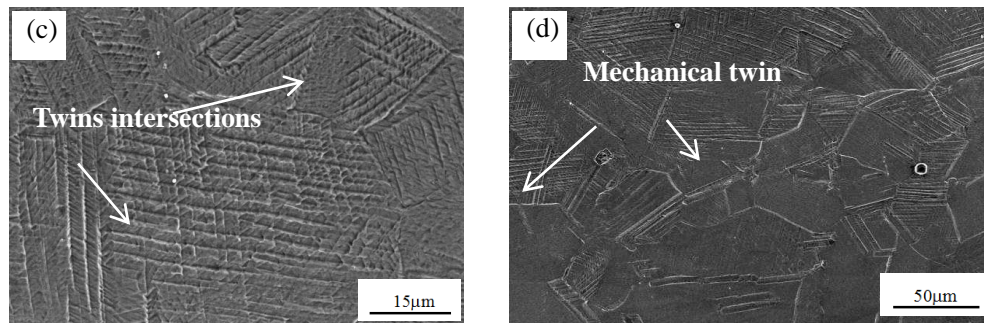


Figure 10. The cross-sectional SEM picture of wet shot-peened for 10 min GH4169 alloy (a); higher magnification of (b) layer A, (c) layer B, and (d) layer C. an increment in the mechanical twin density.

Unal and Varol^[15] reported that mechanical twins and twin intersections could be identified in the highly deformed regions of AISI 304 specimens subjected to severe shot peening because of plastic deformation with high strain rates, which resonates with the results of the present work. Usually, with a decrement in the depth from the top surface, plastic deformation becomes more severe, resulting in an increment in the mechanical twin density. Then, the refined blocks by the intersecting twins become smaller. Plastic deformation promotes twin intersections, allowing for subgrain formation.

The TEM images of layer A in Figure 10(a) and the corresponding selected-area electron diffraction (SAED) pattern are shown in Figure 11. As seen from the images, the SAED pattern consists of nearly complete rings, which reveals that the grains have been broken down into nanosized grains and they show random crystallographic orientations.^[17-18] Additionally, dislocation pile-ups and dislocation cells are observed in the highly impacted surface as indicated by arrows in Figure 11(a), demonstrating that dislocation slip systems are activated, and then, numerous dislocations are formed due to deformation. Figure 12 shows the microstructure beneath the nano-grain layer (layer B in Figure 10(a)). As shown in Figure 11(b), the SAED patterns of the entire region are symmetrical with each other with respect to the $\{1\ 1\ 1\}$ plane, indicating that the original grains have become grains containing twin intersections after wet shot peening. A group of parallel micro- and nano-twins is observed, and dislocations are trapped in those twins. The TEM results confirm that the deformation markings shown in Figure 10(c) are deformation twins due to the identical intersection angle of the markings and twins observed by SEM.

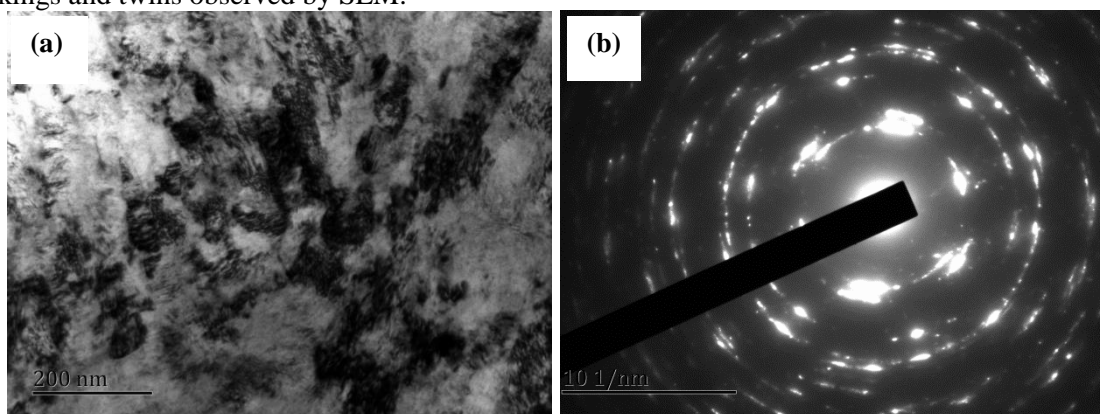


Figure 11. (a) TEM bright-field image of the very surface region in the sample wet shot-peened for 10 min, (b) corresponding SAED pattern.

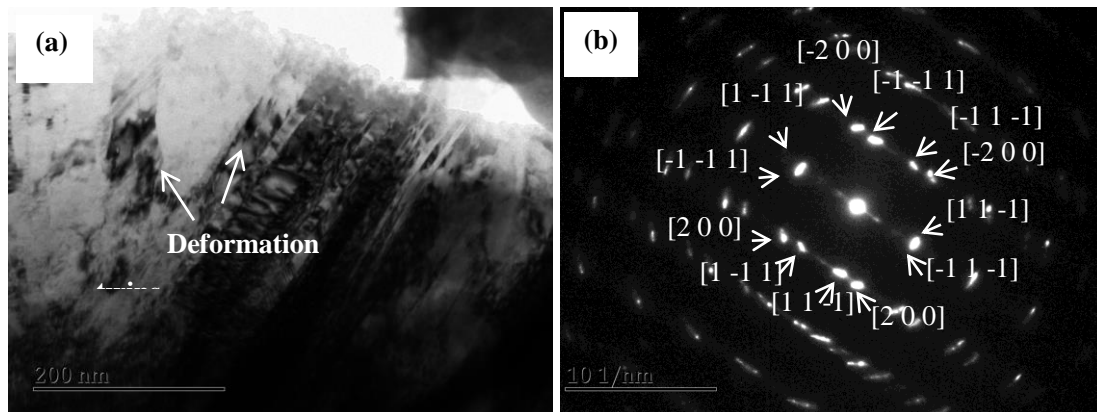


Figure 12. (a) TEM bright-field image of the subsurface region in the sample wet shot-peened for 10 min, (b) corresponding SAED pattern.

The mechanism of grain refinement is related to the stacking fault energy (SFE).^[19] For systems with moderate SFE, such as 316L stainless steel (40 mJ/m²) and Cu (78 mJ/m²),^[20,21] the dislocation activities and deformation may contribute to the grain refinement. Ortiz et al.^[22] studied the microstructure evolution of nickel-base alloys subjected to severe surface plastic deformation. The results showed that deformation twins were far more abundant than deformation faults at any location measured from the impacted surface, suggesting that deformation twinning and dislocations were the dominant deformation mechanisms of the C-2000 alloy under surface impact conditions. In this paper, considerable dislocation activity and massive deformation twins are observed in the surface impacted layer of the wet-treated GH4169 alloy, an fcc alloy with moderate stacking-fault energy (128 mJ/m²).^[19] Hence, the plastic deformation mechanism of the GH4169 alloy may involve dislocation and deformation twinning.

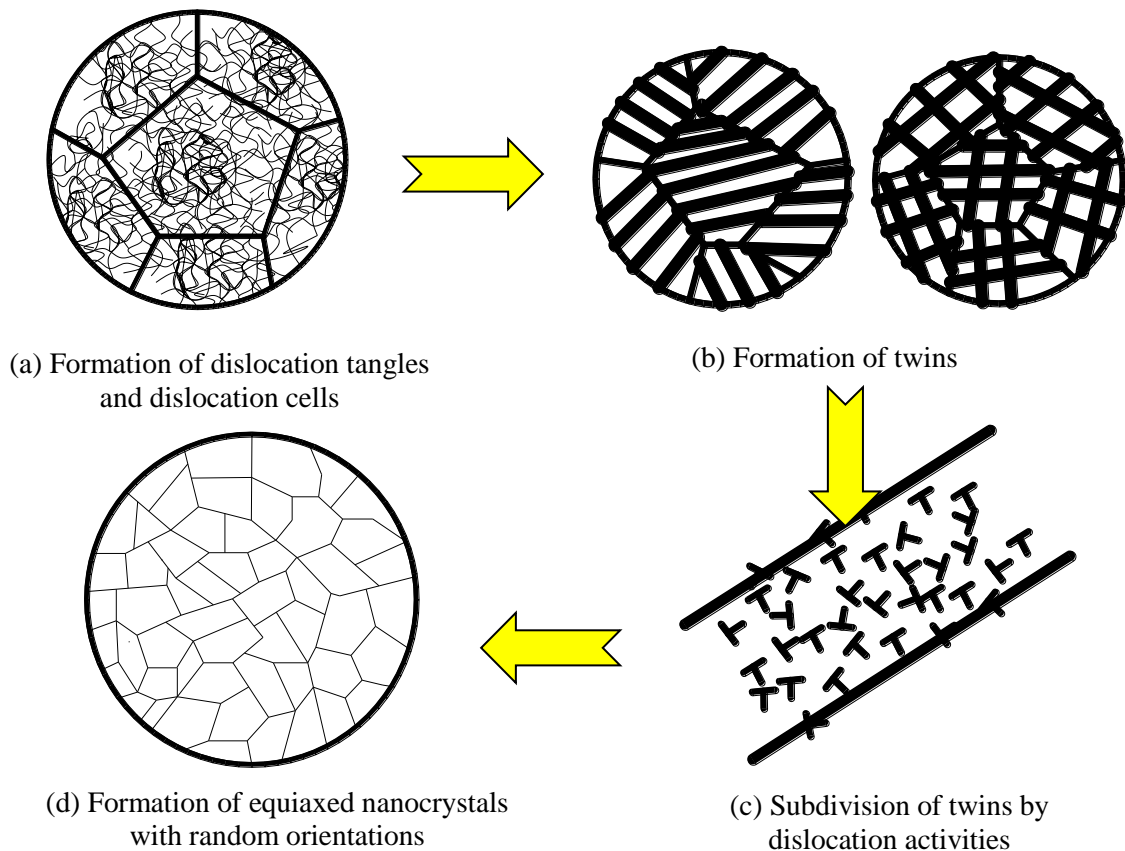


Figure 13 . Schematic illustration showing the microstructural evolution process of GH4169 alloy induced by the wet shot peening.

Figure 13 shows the microstructural evolution of the GH4169 alloy induced by wet shot peening. Usually, the critical shear stress required for dislocation movement is less than that for mechanical twinning under the action of an external load.^[23-24] Thus, a large number of dislocations are primarily generated in the GH4169 austenite coarse grains during wet shot peening. When the dislocation density reaches a certain degree, dislocation cells are formed through dislocation, annihilation, and recombination (Figure 13(a)). With the proliferation of dislocations, stress concentration occurs when a large number of dislocations are blocked, which triggers mechanical twinning, segmenting the coarse grains into lamellar twins (Figure 13(b)). The thickness of the mechanical twins ranges from the submicron to nanometer scale, as shown in Figure 10 and 12. The twins gradually change from lamellar to equiaxed because of the bombardment by shots from multiple directions, due to the motion of the high-density dislocations (Figure 13(c)). Meanwhile, the grain boundary misorientation increases. With the development of dislocations, the grain size decreases and the misorientation increases gradually; finally, an equiaxed and randomly oriented nanocrystalline structure is formed on the surface layer of the GH4169 alloy (Figure 13 (d)).

4.2 Residual stress analysis

A longer processing duration is believed to impart projectiles with higher impact kinetic energy. During shot peening treatment, most of the energy is converted into plastic deformation energy stored in the deformed layer. Thus, with increased time exposure, plastic deformation becomes increasingly severe and more non-uniform, which has a beneficial effect on both SRS and MRS. Chen et al.^[25] studied the effect of wet shot peening on the Ti-6Al-4V alloy treated with ceramic beads. The results showed that the MRS of wet-treated samples appeared in the surface layer, which is quite different

from the results presented here. According to the results in Rosa CEFDL and K.Y. Zhu^[26,27] the actual distribution of residual stress results from the competition of two processes, namely, hertz dynamic pressure and direct plastic extension. MRS would appear in the surface layer as the dynamic pressure becomes minor and plastic deformation is severe on the material surface when the shots bombard relatively soft materials. The steel shots (~250 HV) used in this experiment are softer than those for the GH4169 alloy (~289 HV); the hertz dynamic pressure is dominant, high shear stress appears in the subsurface, and plastic deformation occurs in this region. Hence, MRS occurs in the subsurface layer of the treated samples. Further, the results shown in Figure 9 demonstrate that the MRS of the dry-peened samples is much larger than that of the wet-peened samples. The reason for this may be related to the shot intensity, as it is well known that a larger MRS would be obtained with a higher shot intensity.^[27] In this study, the kinetic energy of the steel shots during the wet shot peening is less than that of the shot at the same speed in the dry treatment, as the lubrication and buffering effects of water decrease the shot intensity. Therefore, the MRS of the wet-treated samples is much lower than that of the dry-treated samples for the same processing duration. Moreover, the residual stress improvement is rather limited with an increment in the processing duration, indicating that the shot peening time may not be an important parameter affecting the residual stress under saturated conditions. Farrahi et al.^[28] suggested that shot peening time is not a significant parameter related to residual stress when the shot is small, and full coverage is reached immediately. In this study, the GH4169 alloy is shot peened by 1 mm shots and full coverage is reached in a short time, as shown in Figure 9.

5. Conclusions

A highly deformed layer is obtained on the surface of a shot-peened GH4169 alloy, and the deformation layer thickness is found to be positively correlated to the shot peening time. The deformation layer of the dry-treated samples is slightly thicker than that of the wet-treated samples, while the surface flatness in the former case is much lower due to numerous craters induced on the surface layer. Dislocation pile-up cells and massive deformation twins occur on the surface impacted layer because of severe plastic deformation, suggesting that deformation twinning and dislocations are the dominant deformation mechanisms of the GH4169 alloy. The surface roughness increases after shot peening, and by contrast with dry shot peening, the surface roughness of the wet-treated samples is much lower due to the lubrication and buffering effects of water. The surface microhardness of the dry peening and wet shot peening surface increased by 20% and 17% respectively. Compressive residual stress is introduced into the surface layer of the treated GH4169 alloy, and the SRS and MRS are -586 MPa and -795 MPa, respectively. The MRS and SRS improve with increasing processing duration, but to a limited extent, as full coverage is reached in a short time. MRS occurs in the subsurface layer because of the dominance of the hertz dynamic pressure. The SRS of the wet-treated specimens is slightly higher than that of the dry-treated samples for the same processing parameters because of the better surface quality. However, the MRS of the dry-treated samples is much larger than that of the wet-treated samples due to the higher shot intensity.

Acknowledgements

This work was supported by the Natural Science Foundation of Jiangxi province [Grant number 20171BAB206006], the Key project of science and technology project of Jiangxi Provincial Education Department [Grant number GJJ160678].

Reference

- [1] Oblak J M, Paulonis D F, Duvall D S, Coherency strengthening in Ni base alloys hardened by DO22 γ' precipitates, *Metall. Trans.* 1974, **5**, 143-53.
- [2] Azadian S, Wei L Y, Warren R, Delta phase precipitation in Inconel 718, *Mater. Charact.* 2004, **53**, 7-16.
- [3] Liu X, Dong J, Tang B, Hu Y, Xie X, Investigation of the abnormal effects of phosphorus on mechanical properties of Inconel 718 superalloy, *Mater. Sci. Eng. A.* 1999, **270**, 190-6.

- [4] Gao Y K, Wu X R, Experimental investigation and fatigue life prediction for 7475-T7351 aluminum alloy with and without shot peening, *Acta Mater.* 2011, **59**, 3737–47.
- [5] Fridrici V, Fouvry S, Kapsa P, Effect of shot peening on the fretting wear of Ti–6Al–4V, *Wear.* 2011, **250**, 642–9.
- [6] Akiniwa Y, Kimura H, Sasaki T, Effect of residual stresses on fatigue strength of severely surface deformed steels by shot peening, *Powder Diffr.* 2001, **24**, 37–40.
- [7] Wen A L, Ren R M, Wang S W, Yang J Y, Effect of surface nanocrystallization method on fatigue strength of TA2, *Mater. Sci. Forum.* 2009, **620**, 545–9.
- [8] Bagherifard S, Guagliano M, Fatigue behavior of a low-alloy steel with nanostructured surface obtained by severe shot peening, *Eng. Fract. Mech.* 2012, **81**, 56–68.
- [9] Feldmann G G, Hennig W, Haubold T, Zinn W, Scholtes B, Comparison of the consequences of shot peening treatment methods on the surface layer characteristics of Ti6246, *Adv. Eng. Mater.* 2011, **13**, 895–900.
- [10] Chen G, Yan J, Tian T, Zhang X, Li Z, Zhou W, Effect of wet shot peening on Ti-6Al-4V alloy treated by ceramic beads, *T. Nonferr. Metal. Soc.* 2014, **24**, 690–6.
- [11] Takemoto M, Shinohara T, Shirai M, Prevention of stress corrosion cracking of weldment by wet shot peening, Balcar G P, The Second International Conference on Shot Peening. *Chicago: International Scientific Committee for Shot Peening*, 1984, **29**, 39–42.
- [12] Sakoda S, Tosha K, Shot peening using wet blasting machine with a wide nozzle, *Adv. Mater. Sci. Technol.* 2009, **614**, 163–8.
- [13] Wang L M, Wang Z B, Lu K, Grain size effects on the austenitization process in a nanostructured ferritic steel, *Acta Mater.* 2011, **59**, 3710–9.
- [14] Zhou L, Liu G, Ma X L, Lu K, Strain-induced refinement in a steel with spheroidal cementite subjected to surface mechanical attrition treatment, *Acta Mater.* 2008, **56**, 78–87.
- [15] Unal O, Varol R, Surface severe plastic deformation of AISI 304 via conventional shot peening, severe shot peening and repeening, *Appl. Surf. Sci.* 2015, **351**, 289–95.
- [16] Darling K A, Tschopp M A, Roberts A J, Ligda J P, L.J. Kecskes, Enhancing grain refinement in polycrystalline materials using surface mechanical attrition treatment at cryogenic temperatures, *Scripta Mater.* 2013, **69**, 461–4.
- [17] Liu W, Zhang C, Yang Z, Xia Z, Microstructure and thermal stability of bulk nanocrystalline alloys produced by surface mechanical attrition treatment, *Appl. Surf. Sci.* 2014, **292**, 556–62.
- [18] Li H, Liu Y, Li M, Liu H, The gradient crystalline structure and microhardness in the treated layer of TC17 via high energy shot peening, *Appl. Surf. Sci.* 2015, **357**, 197–203.
- [19] Tao N R, Wang Z B, Tong W P, Sui M L, Lu J, Lu K, An investigation of surface nanocrystallization mechanism in Fe induced by surface mechanical attrition treatment, *Acta Mater.* 2002, **50**, 4603–16.
- [20] Liu G, Lu J, Lu K, Surface nanocrystallization of 316L stainless steel induced by ultrasonic shot peening, *Mater. Sci. Eng. A.* 2000, **286**, 91–5.
- [21] Wang K, Tao N R, Liu G, Lu J, Lu K, Plastic strain-induced grain refinement at the nanometer scale in copper, *Acta Mater.* 2006, **54**, 5281–91.
- [22] Ortiz A L, Tian J W, Villegas J C, Shaw L L, Liaw P K, Interrogation of the microstructure and residual stress of a nickel-base alloy subjected to surface severe plastic deformation, *Acta Mater.* 2008, **56**, 413–26.
- [23] Lu A, Liu G, Liu C, Microstructural evolution of the surface layer of 316L stainless steel induced by mechanical attrition, *Acta Metall. Sin.* 2004, **40**, 943–947.
- [24] Olson G B, Cohen M, Kinetics of strain-induced martensitic nucleation, *Metall. Mater. Trans. A.* 1975, **6**, 791–5.
- [25] Chen G, Yan J, Tian T, Zhang X, Li Z, Zhou W, Effect of wet shot peening on Ti-6Al-4V alloy treated by ceramic beads, *T. Nonferr. Metal. Soc.* 2014, **24**, 690–6.
- [26] De la Rosa C E F, Trejo M H, Román M C. Effect of Decarburization on the Residual Stresses Produced by Shot Peening in Automotive Leaf Springs. *J Mater Eng Perform*, 2016, **25**,

2596-603.

- [27] Zhu K, Jiang C, Li Z, Du L, Zhao Y, Chai Y, Wang L, Chen M, Residual stress and microstructure of the CNT/6061 composite after shot peening, *Mater. Des.* 1995, **107**, 333-40.
- [28] Farrahi G H, Lebrijn J L, Couratin D, Effect of shot peening on residual stress and fatigue life of a spring steel, *Fatigue Fract. Eng. Mater. Struct.* 1995, **18**, 211-20.